Characterisation of a multi-channel multiplexed EMG recording system: towards realising variable electrode configurations

1st Kylie de Jager
Aspire CREATe, UCL
London, UK
k.dejager@ucl.ac.uk

2nd Michael Mentink
UREST Ltd.
Basingstoke, UK
michael@urest.uk

3rd Henry Lancashire
IDG, UCL
London, UK
h.lancashire@ucl.ac.uk

4th Yazan Al-Ajam
BME, UCL
London, UK
ajam@doctors.org.uk

5th Stephen Taylor
Aspire CREATe, UCL
London, UK
stephen.taylor@ucl.ac.uk

6th Anne Vanhoestenberghe
Aspire CREATe, UCL
London, UK
a.vanhoest@ucl.ac.uk

Abstract—An implantable EMG amplifier with a novel multiplexed frontend for in vivo selection of optimal electrode configurations, was designed using commercially available components. The multiplexers are advantageous as optimal electrode configuration are not known before implantation. The system has 6 ADC recording channels (ADS1298 biopotential amplifier, 2 kHz sampling frequency, 16-bit resolution), and three 8×8 multiplexer arrays (ADG2188), 2 channels per MUX. The system was characterised by measuring input impedance (5.8 MOhm) and frequency response (CMRR 49.0 dB; SNR 51.4 dB). EMG recordings from implanted epimysial electrodes showed lower signal quality (13.5 dB) compared with a commercial EMG recorder (19.5 dB), nonetheless the signals appeared suitable for myoelectric control applications. An implantable version of the EMG recorder, housed within a hermetically sealed ceramic package, should improve signal quality.

Index Terms—Biopotential recordings, electromyography, electrode array, bipolar, tripolar, monopolar, implantable electronics.

I. INTRODUCTION

Socket and strap fitted prostheses are known to cause skin irritation and sores. One possible solution to avoid such complications is to load the bone instead of the skin, through direct skeletal fixation via a permanently inserted bone anchor with soft tissue flange [1]. As a first step towards achieving osseointegrated myoelectrically-controlled prostheses, external EMG recording equipment can be used in combination with a bone anchor conduit [2], through which EMG signals from implanted electrodes can be passed [3].

The quality, or signal-to-noise ratio (SNR), of such EMG recordings is dependent on the electrode configuration to optimise the electrode pick-up area [4; 5]. Al-Ajam et al. [6] proposed incorporating multiplexer functionality in an EMG recording device, which in combination with bone anchor feedthrough, will provide versatility of electrode configurations. This will enable in vivo reconfigurations, increasing the SNR as the optimal electrode configuration changes after implantation.

The design and development of an EMG recorder with a multiplexer frontend, referred to as the CAPITel (Control of Active Prostheses using Implantable Telemetry) system was previously presented in [7]. This paper expands on the earlier work with a thorough system characterisation, in vivo recordings and comparison with a commercial system. The prototype presented was tested as an external device, however

it is designed to be housed in an implantable, hermetically sealed, ceramic package, for use in animal models for further research before implementing the final circuit as an ASIC.

II. METHOD

A. System design and performance evaluation

Figure 1 shows the concept of the CAPITel system (specifications listed in Table II). Multiplexers (MUX), in the frontend of the EMG recorder, allow a variety of electrode configurations from 6-pole electrode arrays, shared between 2 recording channels of a multi-channel analog-to-digital converter (ADC) with adjustable gain. A bandpass filter (BPF), between the MUX and ADC, limits the recorded EMG bandwidth. The digital output is communicated via SPI directly to a micro-controller and via Bluetooth to a laptop for recording. The micro-controller, in combination with a LabVIEW interface,
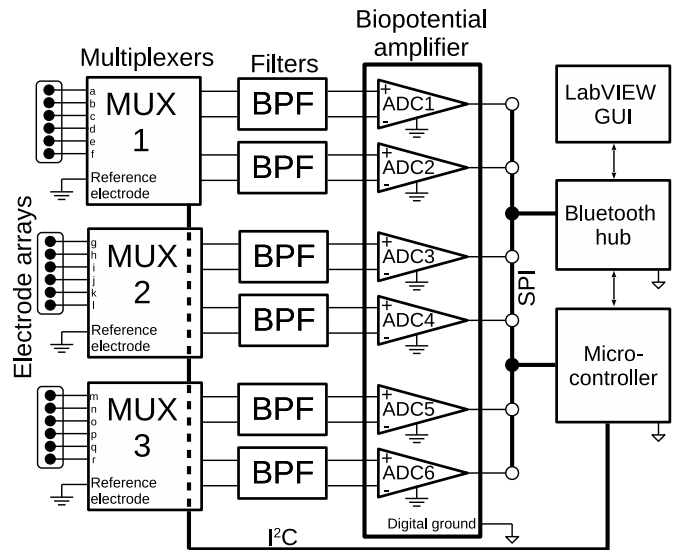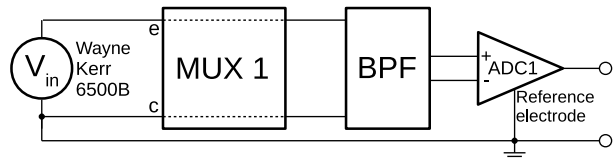

Fig. 1: Block diagram of the CAPITel system showing the frontend MUXs, analogue BPFs and a 6 channel ADC.
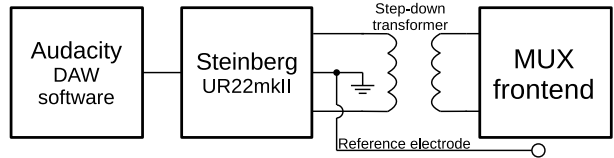
TABLE I: RANDOMISED BIPOLAR CONNECTIONS DURING CHARACTERISATION TESTS.

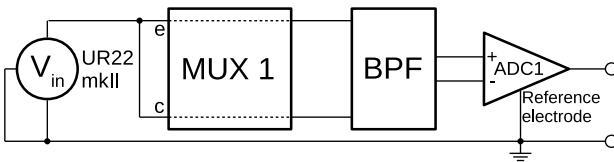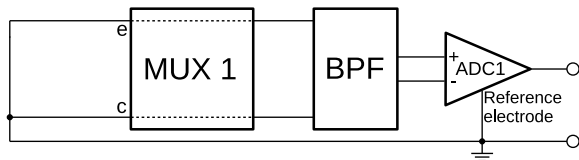| Input terminal	1	2	3	4	5	6
Non-inverting (+)	e	a	j	k	n	p
Inverting (-)	c	d	h	g	m	q

(a) Impedance analyser setup for ADC_1.

(b) Balanced bipolar sine-wave test-bench: Audacity digital audio work station; UR22mkII Steinberg audio interface; step-down transformer.
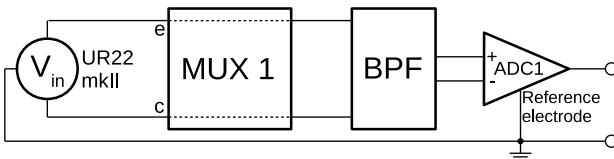
(c) Differential mode setup for ADC_1.

(d) Common mode setup for ADC_1.

(e) Baseline noise setup for ADC_1.

Fig. 2: (a) Test-bench used for system characterisation. (b-d) Internal connections realised with MUX (dashed lines) and external connections for characterising the system impedance, frequency response and SNR of ADC_1. Similar setups were used for each ADC channel bipole connection (Table I).

allows the user to control the ADC gain and define the switch state of the 3 MUXes.

Characterisation tests provide a framework to evaluate the performance of the system. Due to the many electrode configurations realisable with the MUX frontend, each recording channel was characterised for a single, randomly selected, bipolar configuration (Table I).

B. Input impedance

An EMG recording system requires an input impedance greater than 1 MΩ to account for the electrode impedance; Al-Ajam et al. [6] measured epimysial electrode impedances of 2.3 kΩ. A Wayne Kerr 6500B impedance analyzer (20 Hz – 100 kHz frequency range; 1 mA drive current) was used to measure input impedance (Fig. 2a).

C. Frequency response and signal-to-noise ratio (SNR)

Figure 2b shows the test-bench used to generate a balanced bipolar sine-wave test signal (frequency range: 1 Hz – 10 kHz).

This signal was used as both a differential mode (DM) and a common mode (CM) source (Fig. 2c and 2d respectively). The peak-to-peak DM input voltage amplitude (10.6 mV_{pp}) approximates the expected EMG amplitude, while a larger CM input voltage (337.5 mV_{pp}) ensured an output signal was detectable to calculate the attenuation. The internal gain of the ADC channels was set to 6× for all measurements.

For SNR, the baseline noise RMS voltage was measured with the input terminals shorted to the reference potential (Fig. 2e). The RMS voltage measured for the DM source (10.6 mV_{pp} input voltage) was used as the signal RMS voltage.

$$\text{SNR} = 20 \cdot \log_{10}\left(\frac{v_{S,rms}}{v_{N,rms}}\right) \tag{1}$$

D. Power consumption

The power consumption of the system was found by measuring the voltage over a 10 Ω ± 1% resistor, connected in series with the supply line.

III. RESULTS

A. Circuit design

Figure 3 shows the CAPITel circuit, see Table II for design criteria. The core is an ADS1298 ADC biopotential amplifier (6 channels, 16-bit resolution, 2 kHz sampling rate, 1× to 12× variable gain, 500 Hz bandwidth). It has a small footprint (8×8 mm) and low power consumption (6 mW), both necessary for an implantable device. Further benefits of the IC are a low input-referred noise (12.4 μV_{rms}) and wide supply voltage range (digital 5.25 V; analogue 3.6 V).

Three low current ADG2188 multiplexers were used (2 ADC channels per MUX, 8×8 array, 1 μA quiescent supply). Although the ADG2188 has a large footprint (25 mm^2) in comparison to switch-type MUX (3 – 8 mm^2), it saves space by only requiring 2 I^{2}C control lines for all 3 MUX, and the array functionality allows any possible combination of a 6-pole electrode array to be realised.

An analogue bandpass filter (30 – 800 Hz) was incorporated to maximise the SNR. The balanced differential topology minimises the number of components (9 per ADC channel), hence the surface area required on the PCB. Simulations of the filter show an attenuation of -2 dB in the passband.

A MSP430FR2433 micro-controller (126 μA/MHz; SPI and I^{2}C interface; 4×4 mm) communicates with the ADC and the MUX. An external Bluetooth hub (not shown in Fig. 3) transmits the ADC SPI output to a laptop.
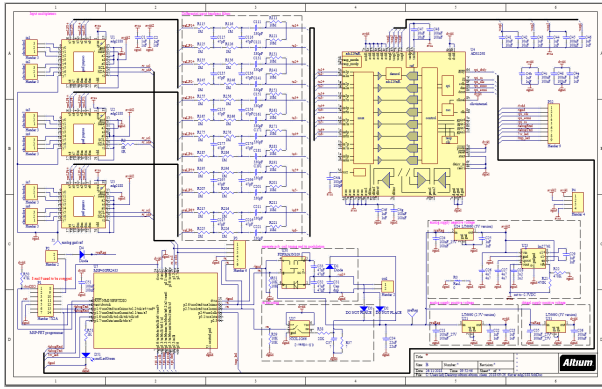
B. Input impedance

Figure 4 shows the measured input impedance (amplitude and phase). Z_{mean} is the average of 12 impedance measurements between the electrode connection pairs (Table I), where one of the pair was connected to ground. This shows frontend impedance to ground (including MUX, BPF and ADC).

$Z_{short-circuit}$, a single impedance measurement between two electrode inputs short-circuited through the MUX, shows the impedance of the MUX.

C. Frequency response and signal-to-noise ratio (SNR)

Figure 5 shows a Bode plot of the differential and common mode gain (A_{DM} and A_{CM} respectively); phase plots have not been included as we could not determine the phase from the digital output of the CAPITel system. The Common Mode

(a) Schematic
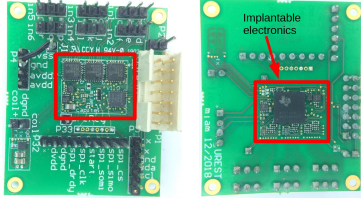
(b) Top layout.

(c) Bottom layout.

Fig. 3: The double sided PCB layout is contained within a 19.33×14.37 mm area (red outline), to be packaged in an implantable, hermetically sealed ceramic housing, in later revisions.
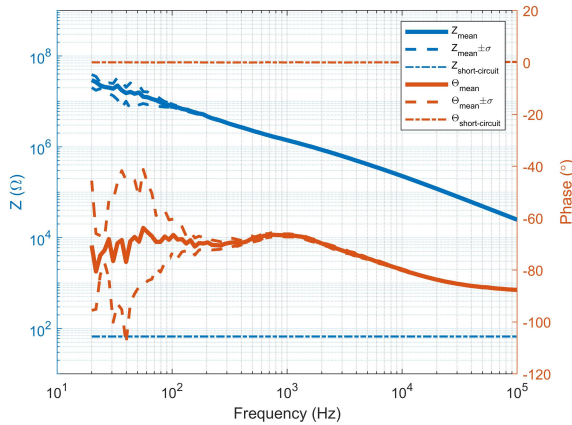

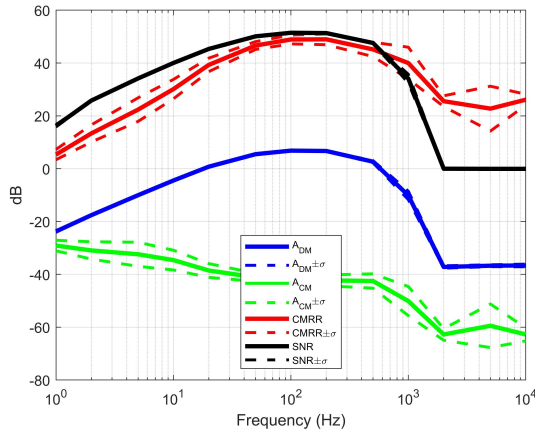Fig. 4: Input impedance and phase measured with a Wayne Kerr 6500B impedance analyser.

Fig. 5: Mean and standard deviation (σ) DM, CM, CMRR and SNR across all six ADC channels. DM, CM and CMRR use V_{pp} values, SNR uses V_{rms} values. Sine-wave test signal amplitudes: DM 10.6 mV$_{pp}$; CM 337.5 mV$_{pp}$.

Rejection Ratio (CMRR) and the SNR are included in the same figure. All four traces are mean values measured with the 6 electrode connection pairs given in Table I. All 6 ADC channels had a gain of $6\times$ during data capture. For the SNR measurements, the DC offset was removed by subtracting the mean from the output voltage, before calculating v_{rms} values.

D. Power consumption

When powering the system with a 5.5 V supply, 8 mA continuous current was measured when idle, increasing to 11.2 mA during data transmission, giving a power consumption range of 44 mW to 61.6 mW.

E. System performance

Table II presents specifications and experimental results.

F. In vivo EMG recordings

Two bone-anchored devices were implanted trans-tibially in an ovine model [6] to provide a hard-wired interface for two epimysial electrode arrays sutured onto the peroneus tertius muscle (5-electrode array) and gastrocnemius (2-electrode array). The CAPITel system realised monopolar, bipolar and tripolar electrode configurations with the 5-electrode array. The same configurations were also realised via a purpose-built switch arrangement [8] connected to a BIOPAC MP150 with EMG100C bioamplifiers (BIOPAC Systems UK, 100 Hz to 500 Hz bandpass, 1000$\times$ gain, 2 kS/s). EMG was recorded with both systems during walking. The CAPITel recordings were post-processed through a second order Butterworth band-pass filter (10 Hz to 500 Hz) for direct comparison with the BIOPAC results.

Figure 6 (a and b) shows the frequency spectrum (FFT) of the EMG (c and d) captured with both EMG recording systems for a bipolar electrode configuration. The signal in the shaded intervals is greater than 1.5 times standard deviation above baseline, considered meaningful EMG activity. Non-shaded intervals were considered to be noise. Equation 1 was used to calculate the SNR for the CAPITel system (13.5 dB) and the BIOPAC system (19.5 dB).

IV. DISCUSSION

The CAPITel system is unique in that it adds multiplexers to an EMG recorder frontend enabling the in vivo selection of electrode configurations. This is advantageous for implanted systems, as: patient-specific optimal configurations, influenced by the exact placement of electrodes on the target muscles, can

TABLE II: DESIGN SPECIFICATIONS AND EXPERIMENTAL OUTCOME FOR THE CAPITEL SYSTEM.

Parameter	Design Criteria	Experimental Outcome
Recording channels	6	6 ADCs (ADS1298)
Sampling frequency	> 1 kHz	2 kHz
Input impedance		
- Z_{mean}	> 1 MΩ	5.8 ± 0.3 MΩ (-70.4° $\pm$ 3.3°)[ab]
- $Z_{short-circuit}$		66.6 Ω (-0.1°)[ab]
Bandwidth	30 – 800 Hz	20 – 500 Hz
Gain (passband)	0 – 40 dB	6.8 ± 0.1 dB[a]
CMRR (passband)	40 dB	49.0 ± 1.9 dB[a]
SNR	>30 dB	51.4 ± 0.2 dB[a]
Power consumption	< 100 mW	44 – 61.6 mW

[a] Measured at 155 Hz; centre frequency of design criteria bandwidth (chosen to prevent contamination from 50 Hz harmonics). [b] Amplitude (phase).
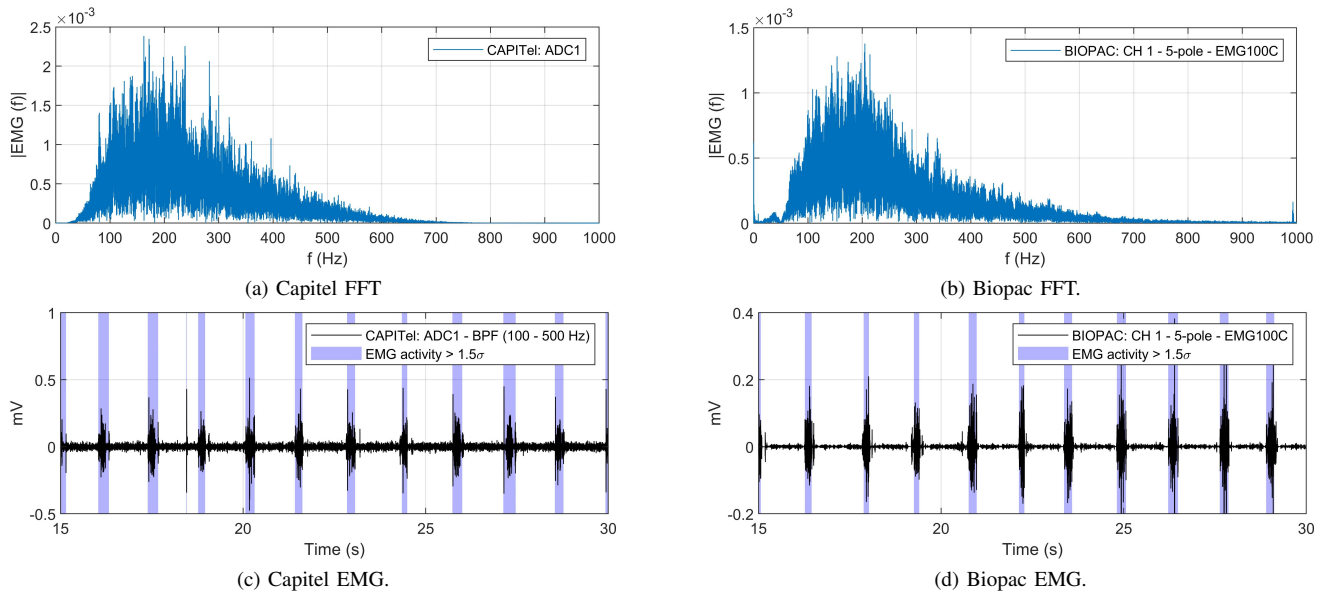
Fig. 6: Comparison of the CAPITel system (a and c) against a commercial BIOPAC EMG recorder (b and d). The CAPITel results were passed through a 100 Hz to 500 Hz bandpass Butterworth filter ($n = 2$) during post-processing to remove DC offset and for direct comparison with the BIOPAC data.

be identified post surgery; and drift in electrode impedance over time can be accounted for without the need for revision surgery.

This proof-of-concept design (fully implantable once encapsulated) was achieved using standard PCB and commercially available components without expensive and time consuming ASIC development.

The presence of the additional frontend components decreases the system performance below that of the ADS1298 (500 MΩ input impedance; 75 dB SNR for a 10 mV sine-wave test signal; 108 dB CMRR at 155 Hz, 5.6 V input signal); CAPITel (input impedance dominated by BPF impedance, 10 MΩ; SNR has 20 dB loss in frontend, MUX and BPF). Some differences are also due to the characterisation test conditions as A_{CM} was measured with an input signal of 337.5 mV_{pp}. Such a payoff is to be expected, but should not deter researchers from utilising encapsulated PCBs when developing implantable prototypes for animal studies as the characterised system still meets the design criteria.

At present CAPITel does not perform as well as the commercial BIOPAC system (section III-F) even after bandpass filtering during post-processing. Nonetheless the signal quality was sufficient for the intended application, namely to identify EMG activity as necessary for myoelectric control.

Further developing CAPITel to realise an implantable EMG recorder will reduce the complexity of implant-prosthesis connection, in this instance reducing from 19 lines (3×6 electrodes + 1 reference) to 6 lines (3 SPI + UART + power + ground). This hard-wired link to power the implant and to facilitate bidirectional serial communications, is feasible in combination with a bone anchor conduit. Applications for which the bone anchor is not suitable, will operate with a wireless link.

V. CONCLUSIONS

An EMG recorder with multiplexing functionality at its frontend was presented. This will allow for in vivo selec-

tion and optimisation of electrode configurations. The performance of the system was characterised by measuring input impedance, frequency response and SNR. The system performed within the required specifications. EMG recordings had lower SNR values compared with measurements captured with a commercial BIOPAC system. Nonetheless, the signal quality was sufficient to detect the presence of EMG activity and will be suitable for myoelectric control of prostheses.

REFERENCES

[1] C. J. Pendegrass, A. E. Goodship, and G. W. Blunn, "Development of a soft tissue seal around bone-anchored transcutaneous amputation prostheses," *Biomaterials*, vol. 27, no. 23, pp. 4183–4191, 2006.

[2] F. Tjulkins, H. Lancashire, K. de Jager, and A. Vanhoestenberghe, "Transcutaneous Feedthrough Enabled Bone Anchor for Attachment and Control of a Smart Upper Limb Prosthesis," in *BioMedEng 2018*, 2018, p. 396.

[3] M. Ortiz-Catalan, B. Håkansson, and R. Brånemark, "An osseointegrated human-machine gateway for long-term sensory feedback and motor control of artificial limbs." *Science translational medicine*, vol. 6, no. 257, p. 257re6, 2014.

[4] T. J. Koh and M. D. Grabiner, "Evaluation of methods to minimize cross talk in surface electromyography," *Journal of Biomechanics*, vol. 26, pp. 151–157, 1993.

[5] J. van Vugt and J. van Dijk, "A convenient method to reduce crosstalk in surface EMG," *Clinical Neurophysiology*, vol. 112, no. 4, pp. 583–592, 2001.

[6] Y. Al-Ajam, H. Lancashire, C. Pendegrass, N. Kang, R. P. Dowling, S. J. G. Taylor, and G. Blunn, "The Use of a Bone-Anchored Device as a Hard-Wired Conduit for Transmitting EMG Signals From Implanted Muscle Electrodes," *IEEE Transactions on Biomedical Engineering*, vol. 60, no. 6, pp. 1654–1659, 2013.

[7] K. de Jager, M. Mentink, F. Tjulkins, H. Lancashire, S. Taylor, and A. Vanhoestenberghe, "A multi-channel multiplexed EMG recording system to study electrode array configuration," in *BioMedEng 2018*, London, sep 2018, p. 367.

[8] H. Lancashire, K. de Jager, F. Tjulkins, and A. Vanhoestenberghe, "Electrode configuration selection for electromyographic prostheses," in *BioMedEng 2018*, London, sep 2018, p. 397.